Chapter 3. Data Availability and Preparation

In this chapter, types of data available for analysis are briefly discussed, with emphasis on the preparation of those actually used in this study. The primary thrust of this work is the use of an optimization technique as applied to ground magnetic data. This optimization technique can in fact be used on any type of data which is able to be represented in digital form and for which a model with variable parameters may be put forward.

a. Fields - Remote and In-Situ

The electromagnetic effects of space plasmas may be measured remotely, primarily from the surface of the Earth, or *in situ*, primarily by satellites. The magnetic field as measured at the surface includes a multiplicity of sources including those from near-Earth space. The electric field at low frequencies as measured there does not include significant contributions from fields in space. Results of satellite measurements of electric fields have been discussed in the introductory chapter, and its role in other modelling techniques will be discussed in Chapter 4. The modelling technique used in this study is based on the magnetic field and does not directly involve the electric field. We proceed by discussing the magnetic field measurement and preparation techniques in detail.

1. Magnetic Fields

Magnetic fields are produced by moving charges or by changing electric fields. As such, they carry information about charge motion (usually differential motion of charges to form electric currents) and about electric fields in a non-static situation. Since they may be detected at great distances from a source, they convey information about distant conditions. This is both an advantage and a drawback in that many sources may contribute to an observed total magnetic field, and it is in practice difficult to disentangle their signals. In the forward modelling approach one attempts to do so by proposing a certain behaviour from known source configurations and matching the data by varying associated parameters.

Magnetic fields also exert pressure, affect charged particle motion, and store energy. These aspects play a role in determining the structure and dynamic behaviour of near-Earth space, as we have seen in previous chapters.

a. Magnetometers

The history of measurement of the Earth's magnetic field in its many aspects is discussed in detail in the monograph by Chapman and Bartels [1940]. The ancient Chinese may be regarded as the first to acquire knowledge of the Earth's field, to the extent that they may have known of magnetic declination [Temple, 1986]. Technical progress in magnetometer design has been substantial since then, and modern systems for measurement of vector magnetic fields to subnanotesla precision are generally based on fluxgate principles [Vacquier, 1993; Forbes, 1987]. In some other types, the total field is determined very accurately while individual

components cannot be measured. These are referred to as scalar magnetometers. In this work it may be assumed that the measurements were taken with fluxgate magnetometers and that the components have been measured to at least 0.1 nT accuracy. Thus, accuracy of the magnetometers is not usually a consideration in error analysis here. Frequently, in fact, data are only stored (and thus available for analysis) to the nearest nanotesla in any case.

b. Ground-Based Magnetometers

Already in the middle of the 19th century, many observatories operated worldwide, largely due to the efforts of Carl Friedrich Gauss (1777-1855). Part of Gauss' motivation in promoting a worldwide observatory network was his mathematical techniques which allowed the separation of an observed field into parts due to internal and to external sources. Given sufficient spatial coverage the origins of the Earth's magnetic field could thus be hoped to be established. Networks of observatories are also very useful in studying the localized and variable fields associated with auroral activity. Figure 3.1 shows data from much of western Canada obtained by the CANOPUS array. Since that time developments in the understanding of the field have been numerous: however it is still the case that further progress is impeded by the sparsity of magnetic observatories. Gauss' goal of understanding the origins of the Earth's main field also has not yet been completely achieved.

In addition to the main field which makes up by far the largest contribution, ground-based magnetometers detect fields due to both external sources and sources within the Earth which are not considered to be parts of its main field. The main field is considered to be of deep origin, has significant spherical harmonic power only up to a certain finite degree and order (that is to say, is spatially fairly smooth), and varies slowly over time. External sources typically have temporal frequencies higher than those of the main field, up to several Hz. Even in polar regions where they may have a large effect on compasses, their magnitude is much smaller than that of the main field. The signals studied here are due to external sources, known to be located in the ionosphere and lower magnetosphere. These are not, however, the only sources of external field in the frequency range considered: the other sources must be considered noise and removed from the data. Sources within the Earth may be essentially DC signals, due to crustal magnetization or local field sources, or may be induced fields arising as a result of variations in the external fields. Local DC signal is generally considered to be an 'anomaly', and may be removed (being DC) by subtracting 'quiet day' signals observed at the same place. Often, however, the presence of a DC anomaly is an indicator of complex structure in the Earth's crust near the station, and these stations also respond anomalously to variations in the field. Such response may aid in modelling the local geological structure, but is inimical to study of processes arising in space. It cannot in practice form part of a forward modelling scheme and here anomalous stations must be treated by a reduced weighting in analysis. Such cases are described where relevant in the analysis chapters which follow. Temporal variations can also occur which are not of interest in studying the currents associated with the aurora. These are now briefly described.

Figure 3.1 Magnetograms from the CANOPUS array for April 11, 1997[1]. The northward component (X) of the magnetic field is shown as a function of UT.

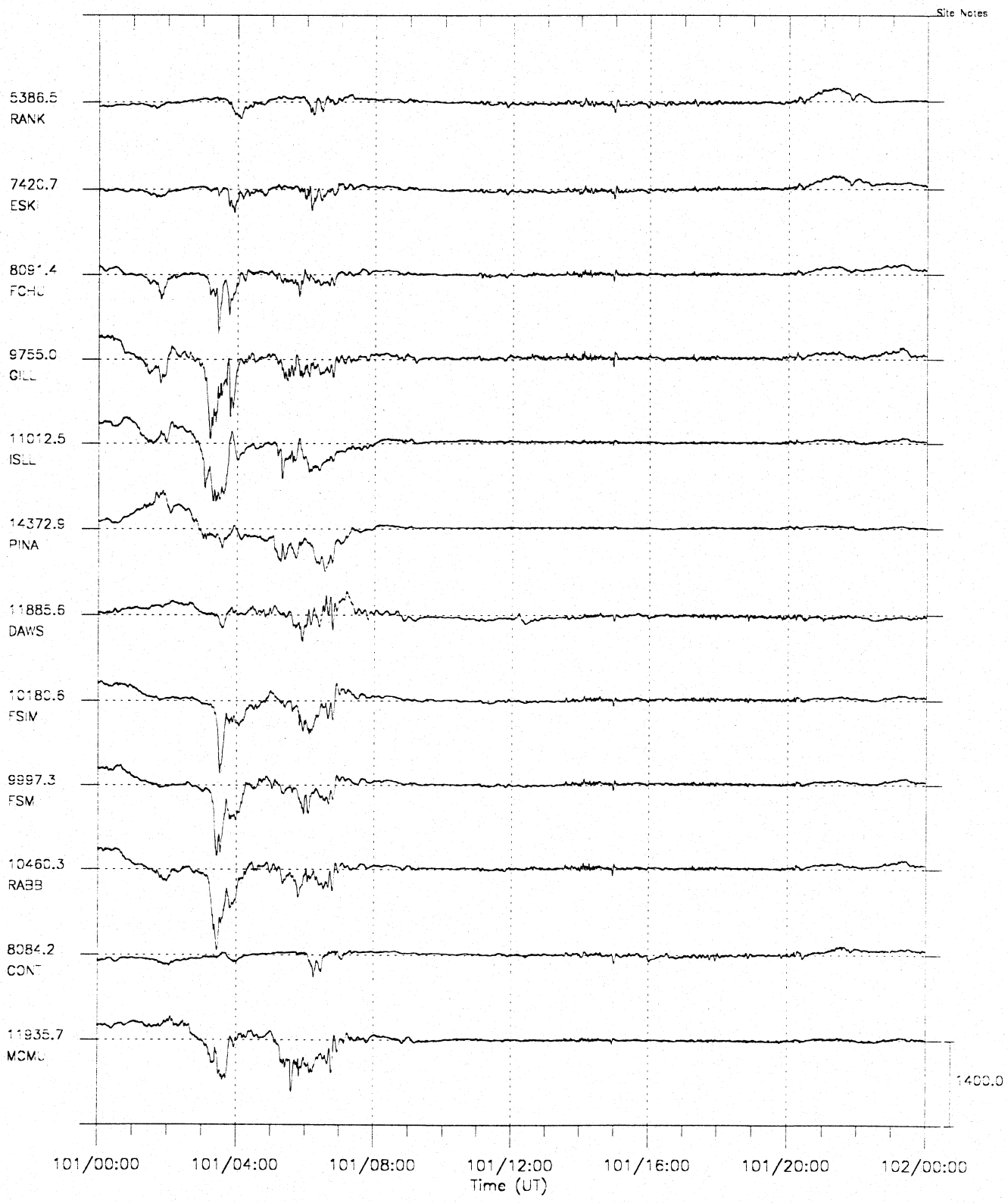

[1] Courtesy of Canadian Space Agency at http://www.dan.sp-agency.ca/www/canopus_home.html

An important source of external signal is the local atmosphere, particularly in daytime. This is primarily manifest in the form of the 'solar quiet' variation, S_q. In response to solar tides and heating, the conducting ionosphere has vertical motion, which induces an electric field since to a good approximation $\boldsymbol{E} = -\boldsymbol{v} \times \boldsymbol{B}$. This field, applied to conducting layers of the atmosphere, in turn causes current flow. This current-carrying layer has been directly observed by sounding rockets although such measurements are few and only of the scalar field due largely to the great difficulty in obtaining precision vector measurements given the poor pointing accuracy possible on a rocket. Observations at midlatitudes by Yabuzaki and Ogawa [1974] showed the current layer to be at 101 to 110 km altitude on a quiet day evening at Kagoshima (31.25° N geographic). Well before the explicit demonstration that an ionospheric current system caused S_q, its equivalent current system was deduced. Now we know that this equivalent current system is in fact a physical current system. Figure 3.2 illustrates the global nature of this current system near equinox, with 25 kA of current flowing between adjacent contour lines. The current is most intense in equatorial regions due to the horizontal orientation of the main field there and greater tidal and heating effects on the atmosphere. The system is approximately centred on noon local solar time; at this equinoctial time it is also centred on the equator. At other times of the year the overall system moves latitudinally with the Sun: further north in summer and further south in winter (Northern Hemisphere seasons). As observed from the ground the S_q variation has latitude dependence and local time dependence as would be expected from the location of the current systems. Figure 3.3 shows the behaviour of averaged S_q at various latitudes. Tashkent, at 69.3° E, 41.4° N (geographic coordinates), is illustrative. As the day progresses, it is carried to larger local times, first passing under a region of essentially southward ionospheric current flow which produces a ground magnetic perturbation which is mainly eastward, or in the sense of positive Y. Thus the Y trace here shows a prenoon maximum. At local noon the overhead current flow is essentially westward producing the noon minimum in the X or northward magnetic component. For postnoon local time the overhead current flow is essentially northward and a Y minimum is seen. The X or northward component is maximal when east-west current is overhead, which is at local noon, and varies in amplitude with the latitude of the station. Stations at approximately 30° latitude show little variation in the north-south component as east-west currents do not pass overhead. These stations do see ample Y or eastward component as they rotate under the Sun. Depending on the hemisphere, first one sign and then the other of north-south current flow passes overhead. Since the overall half-width of the system, as seen in Figure 3.2, is about 90° of longitude or 6 hours of local time, the Y component extrema are separated by about this amount of time. Figure 3.4 shows total Y magnetic variation at Fredericksburg, geographic latitude 40° N, during the UT day of April 3, 1986 (see chapter 6 for a thorough analysis of part of this day) and on another April day. Local noon at this station is at roughly 17 UT and Y component variations peak at roughly 14 UT and have minima at roughly 19 UT. This behaviour is consistent with that described above, and the figure may be compared to the Y component curve at Tashkent in Figure 3.3 given the comparable latitude. Also of note is that the April 3 data show large perturbations at 0 to 8 UT which are not present on the quieter day. These occur in local night, and the quiet day shows that S_q effects, as expected, are minimal during this time

period. However, while the perturbations in question are large compared to what is usually seen, they are of approximately the same size as the S_q variation. If dayside data are used, then, it is clear that S_q effects must be allowed for in some fashion. This is usually done by simple subtraction from the studied perturbations of those of a quiet day not more than a week or so from the day being studied. Since S_q varies with season, a quiet day too far removed in time from the day studied would introduce spurious S_q effects or not sufficiently remove those present. This technique assumes that the S_q variation is not much affected by the processes responsible for the disturbance being studied. In practice, this method of reference to a quiet day has been used in most data preparation in this study. Another method for S_q removal is to grid S_q as a function of known variables such as day of year, location, and local time and remove this function appropriately evaluated. This approach removes, by averaging, random effects which may be present on any given quiet day. Once more the implicit assumption is that the quiet day variation removed is appropriate under the conditions studied.

Figure 3.2 S_q ionospheric current system under equinoctial conditions. 25 kA flows between each adjacent pair of contour lines, with direction of circulation shown by an arrow in each hemisphere. The system, fixed in local time, causes varying perturbations as a station passes under it with Earth rotation. From Parkinson [1983].

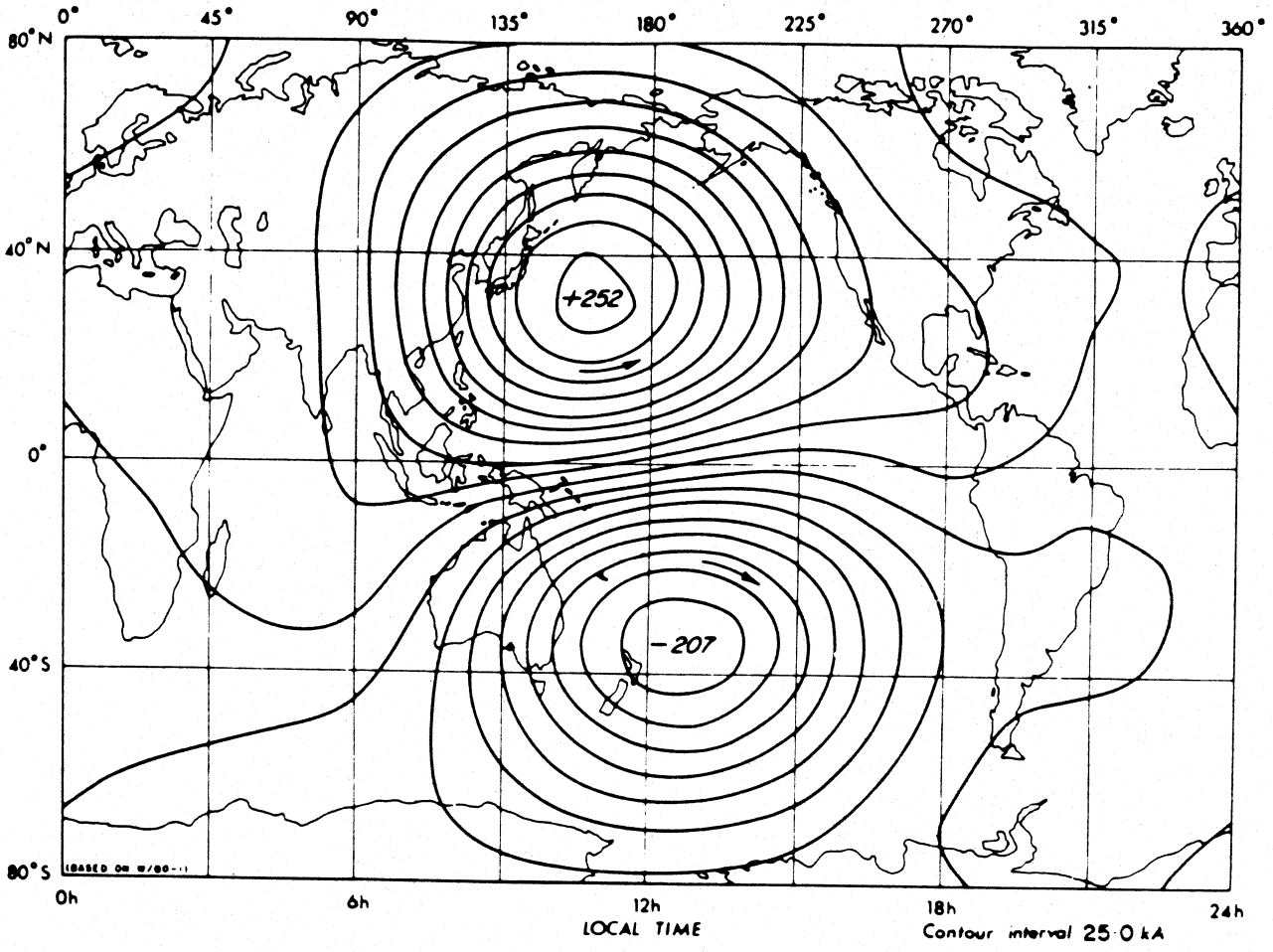

Figure 3.3 Averaged quiet day variations at various latitudes, showing principally S_q variations. Local time is indicated under each stacked component as M (midnight) or N (noon). From Parkinson [1983].

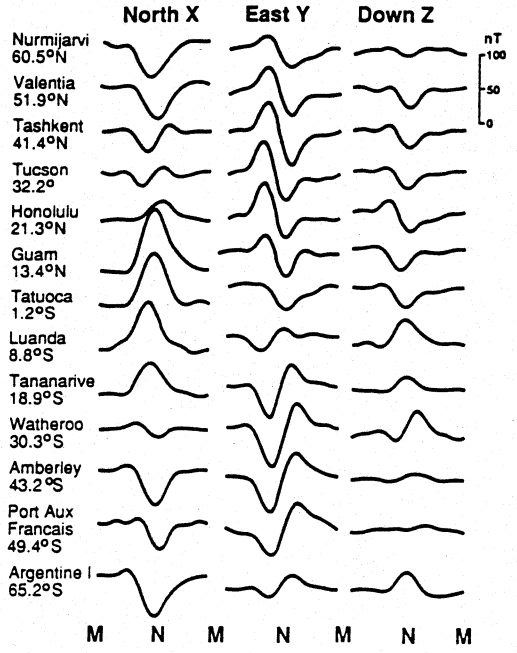

Figure 3.4 Perturbations observed at Fredericksburg (77.5° W, 38.3° N geographic), showing total Y component on April 3, 1986 (solid line) and on a quieter April day (dashed line).

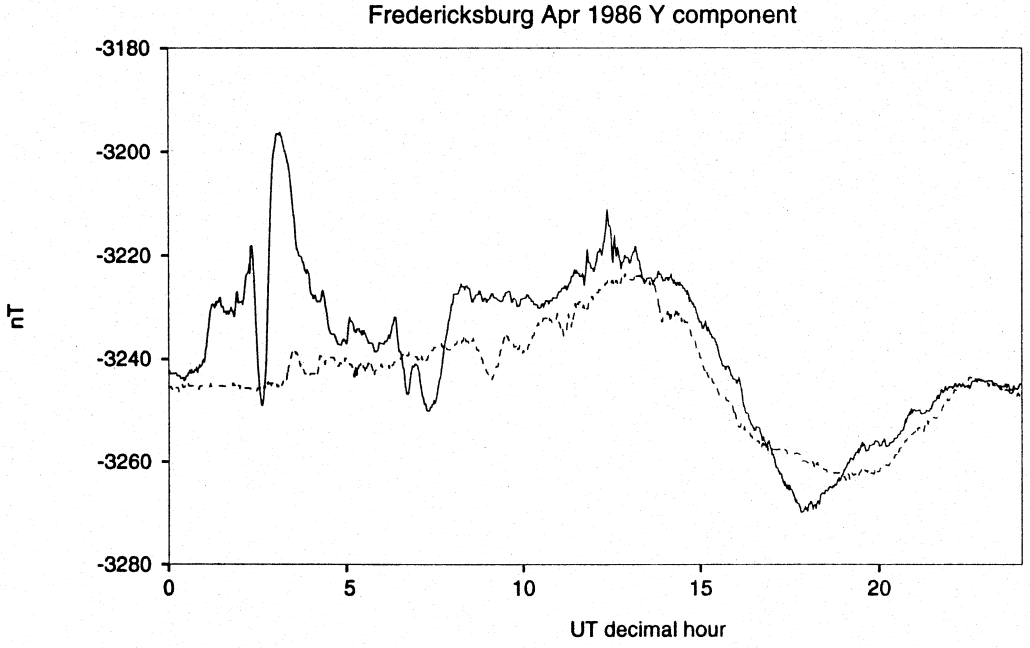

It is implied above that nightside data do not need to be corrected for S_q, although this might depend to a certain extent on the season. In some cases it is most practical to work with only nightside data and to choose a quiet interval as a reference point. There may be little choice, as campaign or study interval data such as those of CDAW may not include appropriate quiet intervals in the data set. Figure 3.5 justifies this approach by showing data from Soroya in Northern Scandinavia (22.8° E, 70.6° N geographic) taken from the CDAW 9 data set and referenced to a baseline value from 20 UT April 2 1986. At 1:05 UT on April 3 1986 each data line has its corresponding value, as corrected by comparison to a quiet day (April 4, 1986) and averaged over 5 minutes, shown by a filled circle [B. Emery, personal communication, 1995]. It is seem that in this case simple removal of a reference value during a quiet interval on the same night has produced an accurate representation of the perturbations. As this station is roughly one hour of local time ahead of Greenwich, night hours are from about 17 UT to 5 UT. S_q effects should be mainly near local noon (11 UT, just off the diagram) in the north-south component at this latitude (compare figure 3.3) but are not easily seen in the data shown. They are typically small, while substorm-related variations are large, at auroral zone stations, particularly on the nightside. However, the method used in this study attempts to include global stations, including those at middle and low latitudes. For some of these, particularly on the dayside, S_q removal by one of the methods described is important.

Figure 3.5 Comparison of magnetic perturbations deduced from two methods of correcting night time variations. Lines indicate the H, D, and Z components (solid, dashed, and dotted, respectively) for April 2-3 1986, as referred to 20 UT April 2. Filled circles indicate data points at 1:05 UT as corrected by reference to the April 4 1986 quiet day. The two methods have produced comparable results at 1:05 UT.

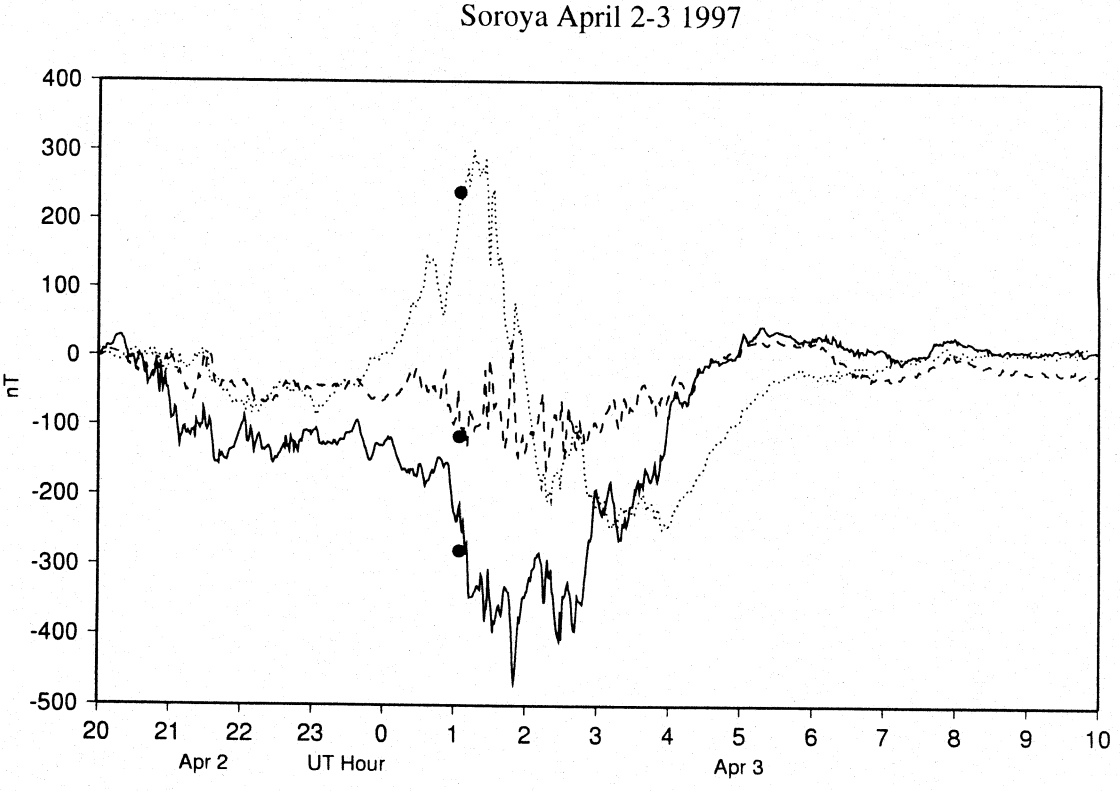

Since the magnetic field is present throughout three-dimensional space and variable in time, visualizing it is difficult. Representation in various graphical forms, notably as stacked magnetograms as in Figure 3.1, may be useful (other forms were explored by Kisabeth [1972]). Modelling, either through purely mathematical expressions, or through parameters having some physical meaning, may also be helpful simply to aid in data display. Another method to facilitate use of ground data from many locations is though an appropriate magnetic index. The use of indices, such as D_{st} referred earlier, has been widespread. For auroral zone perturbations, the auroral electrojet (AE) index has been the most widely used single number giving an indication of global activity. AE is based on superposition of H perturbations from many observatories. The index is produced as a difference of outer envelopes of the most positive and most negative perturbations from all of the observatories involved. The outer envelope of the most positive perturbations is referred to as AU (U for 'upper') and that of the most negative as AL (L for 'lower'). In active times AL is often strongly negative and dominates, so that AE in such cases is comparable in magnitude to AL, but positive. Clearly, since the auroral electrojet indices are outer envelopes only, much information is lost even from the H component in forming the index. Also, the other components are not incorporated into the index. What has been discussed here can be applied to produce indices from any set of stations. In practice, 12-station auroral electrojet indices based on certain stations spaced roughly 2 hours of local time apart, and all at roughly the same magnetic latitude (65°), are widely used. Unless otherwise specified, auroral electrojet indices are taken to be based on the above procedure applied to the standard stations, whose locations are shown in Figure 3.6.

Figure 3.6 Locations of the 12 standard auroral electrojet stations.

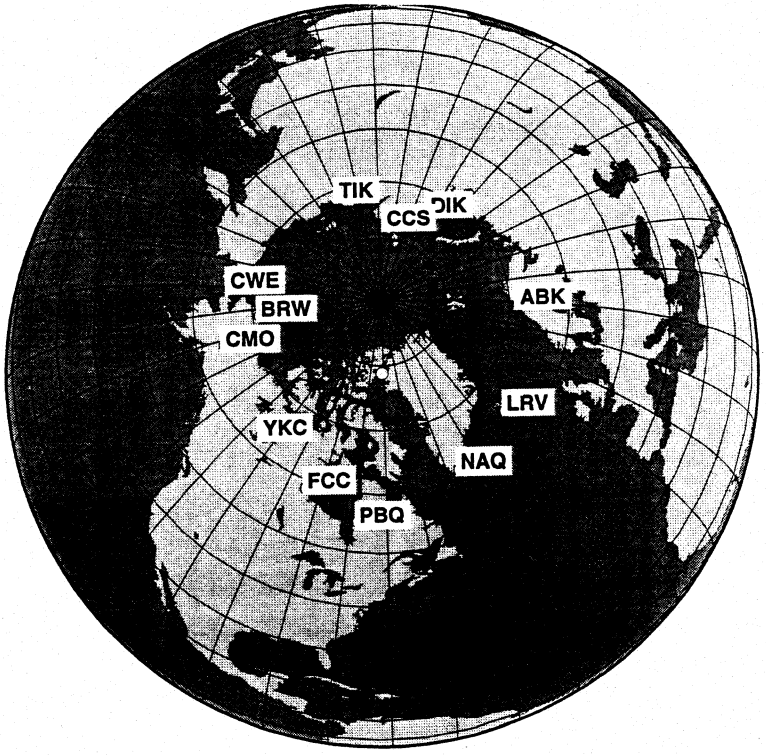

c. Spacecraft Magnetometers

The advent of Earth-orbiting satellites in 1957 opened the possibility for *in situ* investigation of the magnetic field in near-Earth space. Initial investigations by the Explorer 1 and 3 satellites in 1958 used the effect of the magnetic field on trapped high-energy particles to explore its geometry [Burrows, 1990, pp. 79-80], although direct field measurements were not done by these spacecraft. The first spacecraft magnetometer flew in 1958 and by 1961 vector measurements were being taken [Parks, 1991, Chapter 3]. Very soon it was realized that the field in near-Earth space was not completely dipolar: 1961 measurements from Explorer XII led to the discovery of the magnetopause. Slightly later, Ness and coworkers [see again Parks, 1991] observed abrupt reversals in magnetic field direction best explained by the presence of a tail current sheet. Large amounts of spacecraft data have been gathered in intervening years and have contributed to our view of the large-scale structure of the magnetosphere, especially when interpreted in conjunction with other data sets. Some of these data, from magnetospheric spacecraft on distant orbits, such as ISEE (recall Figures 1.15 and 1.16), have already been briefly discussed. An example of behaviour at synchronous orbit has also been shown (Figure 1.20) and the continuous presence of satellites at this location for Earth monitoring has produced important data sets. In conjunction with surface modelling, however, the low Earth orbit class of spacecraft is important and data from this class (typified by Triad, already discussed above) will receive the most attention here.

Recent low Earth orbiting spacecraft carrying magnetometers have included Viking and DMSP F7. Viking operated line-of-sight to Sweden and was generally at about 2 R_E (13500 km) altitude when producing images. Although calculation of the magnetic footprint is straightforward, this high altitude is not favorable for examination of small-scale structure of field-aligned currents in the near-Earth region. This region is better explored by low altitude spacecraft such as DMSP F7 which may nominally be considered to make polar passes at about 800 km altitude (similar to Triad) and thus to respond mainly to field-aligned currents near the ionosphere [Lopez *et al.*, 1991] and somewhat to ionospheric currents.

The satellites of the Defense Meteorological Satellite Program (DMSP) are a series of low-altitude (835 km), polar-orbiting (98.7 degree inclination) satellites. The orbital period of 101 minutes makes the satellites Sun-synchronous. To a large degree, the magnetosphere is also aligned with the Sun-Earth line and a Sun-synchronous satellite samples an equivalent region on each orbit. There are normally two DMSP satellites operating at a time; one in a 0600-1800 local time (LT) orbit and one in a 1030-2230 LT orbit. During the CDAW events modelled in subsequent chapters, DMSP F7 was in a 1030 LT orbit. Its companion F6 was in a 0600 LT orbit but did not carry a magnetometer. The primary purpose of the DMSP satellites, as military weather satellites, is to observe the tropospheric weather using a 2.8 km resolution visible and infrared imaging system. Incidental to this primary mission is the observation of aurora under suitable activity and lighting conditions (see section 3.c.3).

Magnetometer data as supplied [F. Rich, personal communication, 1994] are in ASCII form in logical groups of one minute. The data are almost continuous, with occasional gaps of a few seconds to a few minutes due to telemetry errors. There are a few gaps of hours due to malfunctions at tracking stations, corrupted raw data tapes, and miscellaneous problems. Ephemeris information was supplied for the start of each one minute of data and intermediate positions were calculated as a function of time using splines [Press *et al.*, 1992, Section 3.3]. The ephemeris gives the date and time at the beginning of the minute, the position of the satellite (in fact the footprint traced down magnetic field lines) at this time in geographic and corrected geomagnetic coordinates, the model magnetic field vector (nominally IGRF 80, but in data used here a provisional IGRF 1983.5 was used [F. Rich, personal communication, 1994]) in spacecraft coordinates, and the number of seconds of data in the associated data file. The data file has up to 60 records (or lines) per minute. Each record gives the second of the minute and the 1-sec average of the difference vector (measured magnetic field minus model field). Invalid data were marked by subtracting 1.E6 from the sample. The raw data contained 20 vectors per second. Data supplied for this study were from the standard database and included data from only magnetic latitudes greater than approximately 48 degrees (although the raw data base contains data from all latitudes). Data were supplied in a coordinate system with one component parallel to the spacecraft velocity vector, and for use here required rotation about the vertical into an Earth-fixed coordinate system.

The spacecraft coordinate system has:
+X downward along the local vertical;
+Y perpendicular to +X, in the orbit plane roughly parallel to the velocity vector; and
+Z perpendicular to +X and +Y and parallel to the orbit plane normal.
Transformations were performed from this coordinate system into Earth-centered systems using ephemeris data. The spacecraft velocity vector must be accurately determined for such transformations. It was found that interpolation in the one-minute ephemeric table produced uncertainties in the pointing direction with period of about one minute. Such uncertainties in turn produce spurious variations in the transformed magnetic data which are comparable in effective spatial extent to those associated with the auroral zones. Thus a rough orbital fit based on the extremal latitude attained on any given orbit was preferred. An effective orbital inclination derived from this allows a fit with very smooth variation of the spacecraft pointing angle and no spurious effects due to inclination.

The body-mounted (as opposed to boom-mounted) fluxgate magnetometer flown on the DMSP/F7 satellite was a proof-of-concept instrument. The magnetometer returned data on the near-Earth field from December 1983 to October 1987. Numerous spacecraft background signals are present in the data, as will be seen and discussed in data analysis chapters. The magnetometer has been evaluated as almost, but not quite, good enough for modelling the main geomagnetic field [Ridgway *et al.*, 1989]. In practice, use of the data in an absolute sense is not necessary in this study, and the near-repeatability of the orbits favors an approach in which a quiet day is used as a baseline, rather than use of an absolute baseline based on the subtraction of the main field appropriate to the spacecraft location. The subtraction approach was attempted, using the appropriate IGRF model, but

did not yield satisfactory results. Such baseline problems are not restricted to this study: DMSP data has been little used (perhaps underused) due to them, and recently an attempt has been made to obtain better magnetic data from this satellite series [F. Rich, personal communication, 1995].

Figure 3.7 illustrates artifacts in the DMSP/F7 magnetometer data during a northern hemisphere pass on April 4 1986, which was geomagnetically quiet in the early UT hours during which the pass occurred. No strong features attributable to natural currents are evident in this plot. The strongest features are artifacts. On the bottom half of the curves, at approximately 65° geomagnetic latitude, is a level shift likely due to tape recorder activity (most but not all of these are removed in processing). On the top (nightside) portions of the curves at 60° to 62° is a signature clearly associated with shadow entry and visible on all passes examined at this local time. Apart from the likely shadow entry signature, the changing of background levels with position of the spacecraft is not explained here: rather the levels as presented are taken as quiet time repeatable levels and used as a basis of comparison (i.e. baseline) when these data are analysed. Data used in this manner allow determination of the locations and strengths of current systems; further, the perturbations may be correlated with particle data available from the same spacecraft at the same time. That is not done in this study, which is focussed on magnetic data.

Figure 3.7 Geographic X (solid) and Y (dashed) components observed by the DMSP/F7 magnetometer on April 4 1986 on an early UT northern hemisphere pass. Bottom portion of each curve corresponds to dayside.

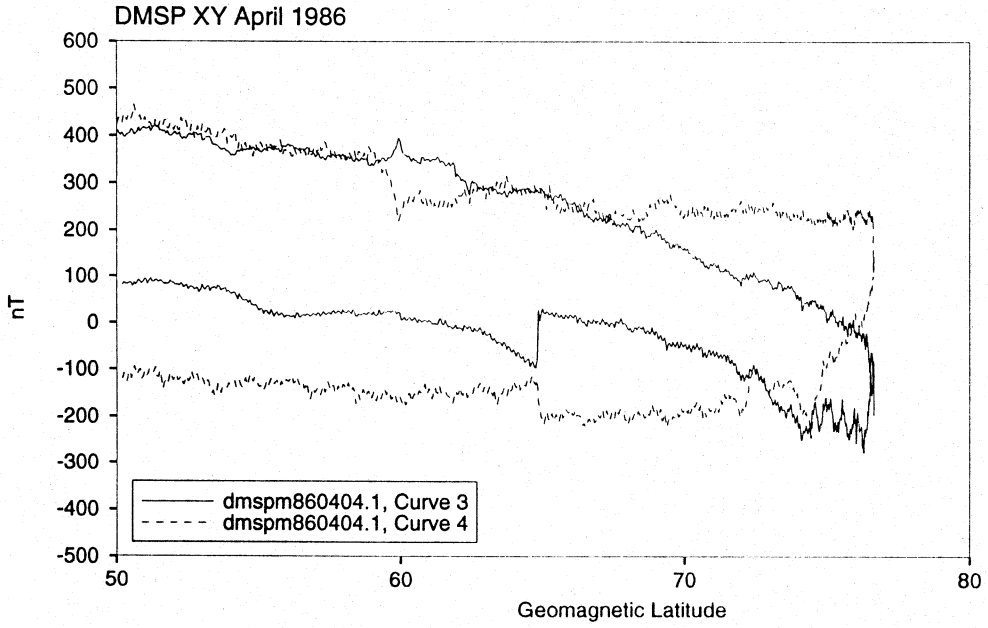

As alluded to in Chapter 1, the magnetic field of the solar wind is also an important quantity in the solar-terrestrial interaction. Since 1973 (October 26 launch date) the IMP-8 spacecraft has been the 'workhorse' at measuring properties of the near-Earth solar wind [King, 1982]. During its period of about 12.5 days, the spacecraft is typically in the solar wind about 60% of the time, and is between 25 and 45 R_E from Earth. Its data are sometimes used in magnetospheric studies while it is in the tail. Although the data are now available in near-real time[2], the chance of the spacecraft being in the solar wind is no longer the limiting factor in obtaining its parameters. The acquisition of data from the spacecraft is now sporadic, presumably for operational reasons. More remote from Earth but always in the solar wind, and with data almost constantly received as of this writing (summer 1997), the WIND spacecraft now provides valuable solar wind data[3]. WIND was launched on November 1, 1994 and is at the Earth-Sun L1 Lagrangian point. At typical solar wind speeds this provides one hour 'warning' of active conditions upstream, but in timing studies the temporal offset, far more than that from IMP-8, is a disadvantage. IMP-8 and WIND measure various plasma properties in addition to the magnetic field.

b. Particles

Since auroral emissions are largely due to precipitation of energetic particles into the upper atmosphere, particle detectors on satellites can provide information about aspects of auroral phenomena. Interpretation of particle data can lead to inferences about resulting ionospheric conductivity [Knipp, 1989] and about magnetospheric source regions. The primary purpose of examining particle data in the present study is to assist in locating auroral features and for this the low altitude data from DMSP are most useful. In some cases, particles will be discussed in other contexts. These include detection of injected energetic particles in synchronous orbit as a result of substorm activity, and use of particles as diagnostic indicators of spacecraft residence in certain areas of the magnetosphere.

The following description of DMSP particle detectors is based on descriptive computer files from the National Geophysical Data Center. The DMSP particle detector, SSJ/4, provides a high dynamic range energy spectrum of the low (typically keV) energy particles that cause the aurora and other high latitude phenomena. The SSJ/4 instrument was designed to measure the flux of charged particles as they enter the Earth's upper atmosphere from the near-Earth space environment. It consists of four electrostatic analyzers that record electrons and ions between 30 eV and 30 keV as they flow past the spacecraft toward the Earth. The instruments "look" toward the satellite zenith. The curved plate detectors allow precipitating electrons and ions to enter through an aperture. Electrons and ions of the selected energy are deflected toward the target by an imposed electric field applied across the two plates. The two low energy detectors consist of 10 channels centered at 34, 49, 71, 101, 150, 218, 320, 460, 670, and 960 eV. The high energy detector measures particles in 10 channels centered at 1.0, 1.4, 2.1, 3.0, 4.4, 6.5, 9.5, 14.0, 20.5 and 29.5 keV. There is effective overlap of the highest of the low-energy

[2] http://ndads.gsfc.nasa.gov/ndads/archives_form_IMP8.html
[3] http://www-spof.gsfc.nasa.gov/istp/wind/wind.html

channels and the lowest of the high energy channels. At high counting rates these detectors are found in practice to produce near-identical counts [F. Rich, personal communication 1994]. Differential particle fluxes (in units of electrons/cm^2/s/steradian/eV) may be as large as 10^{10} at the lowest energies. The detectors also record high energy ions that penetrate both the satellite and the instrument but discussion of particle data here is qualitative and this is not considered further. Each detector dwells at each channel for 0.09 seconds from high energy channel to low. A complete cycle is sampled each second. In this study the particle data were combined with positional data obtained from ephemeris files as described in the section on satellite magnetometers.

Particle data from synchronous orbit is primarily available from the GOES series of spacecraft and from Los Alamos sensors on military spacecraft. The GOES Energetic Particle Sensor (EPS) is part of a standardized package known as Space Environment Monitor (SEM) carried on GOES and other spacecraft since the 1970s [Fritz and Neely, 1982]. The EPS aims mainly to detect high energy particles (protons and alphas) of external origin but some trapped particles are also detected (high energy electrons of 2 MeV or more and the lowest energy proton detector band of 0.6 to 4.2 MeV) [Wilkinson and Ushomirskiy, 1994]. The Los Alamos instrument package is sensitive to electrons and protons in lower energy ranges, which are primarily trapped. Substorm injection of such particles is well known and was referred to in Chapter 1. The instrument is described by Baker *et al.* [1982] and an example of proton injection associated with a substorm onset, and subsequent drift echoes, is presented there.

Figure 3.8 Dispersive injections of protons into the synchronous orbit region. Observations are from the ATS 5 particle detectors. Energy increases downward on the main plot. The AU and AL indices are shown; large AL bays are highly correlated with extrapolated infinite energy injection times. The D_{st} index is also shown.

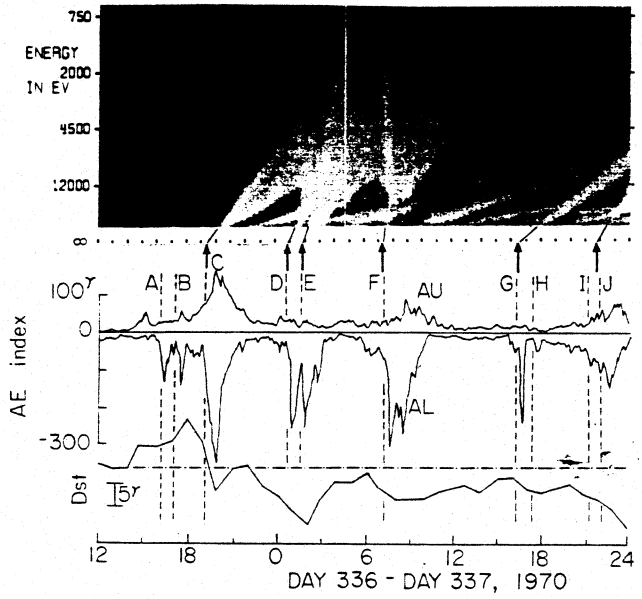

Figure 3.8 illustrates proton injections and their association with substorms as deduced from the AE index and Dst (partially, at least, caused by the injections) in an early study by Kamide and McIlwain [1974]. The injections as observed at the spacecraft (ATS-5) are generally dispersive due to their being associated with midnight sector activity, the differential drift velocity of protons depending on energy, and the fact that the geostationary satellite is not continually near the midnight sector. The one injection with little dispersion is labeled 'F' and this was observed when the spacecraft was very near the midnight sector. In the more general case the spacecraft was not near the point of injection, and the near-linear increase in particle velocity (approximately 15.2 E L^2 ms^{-1} westward for protons with energy E keV bouncing near-equatorially at radius L Earth radii [Lyons and Williams, 1984, p. 25]) with energy means that the most energetic particles arrive first at the spacecraft, followed by less energetic particles. Extrapolating the curves of arrival versus energy to infinite energy allows approximate determination of the injection times. In several instances in the analysis chapters of the present study, injections as observed by synchronous spacecraft at various longitudes prove useful in localizing and timing substorm onsets.

c. Imaging

Auroral imaging has traditionally been done with ground photography. Photographic triangulation allowed the establishment of the altitude of auroras as being above about 100 km. All sky imaging, in which an optical system produces an image of the entire dome of sky visible from a site at any given time, is useful in establishing the larger scale relationships among auroral features. With several such imagers, the scale may be extended to be nearly global, as exemplified by the pioneering work of Akasofu [1964]. Here, however, few all sky images will be referred to, partly due to the availability of satellite images at times of interest.

Only since the 1970's has it been possible to image the aurora from above using satellite-mounted cameras. A wide, sometimes global, field of view from one instrument is an important advantage of satellite imaging. Correlation between forms may be done without the obstacle of the local horizon. Further, the restriction to observing radiations which pass through the Earth's atmosphere is lifted, although there may still exist absorption or scattering between the emitting layers and the spacecraft.

Another imaging technique which attempts to use the electromagnetic spectrum effectively is meridian scanning photometry [Rostoker *et al.*, 1995]. Although viewing is restricted to one dimension, generally several spectral lines are imaged simultaneously. Auroral behaviour at several wavelengths, through time and along the scan dimension (the meridian) can be effectively displayed. Meridian scanning photometry from the CANOPUS array is used in a demonstration study with CANOPUS data in Chapter 9. It is noted here, but will not be demonstrated, that the fitting technique used for magnetic data in this study could be readily applied to meridian scanning photometer data.

The images most used here are those produced by the Viking spacecraft, which flew in 1986. These have the advantages of good spatial and temporal resolution (since exceeded by the Freja spacecraft). Viking's constraints of narrow field of view and rapid polar passes do not affect this study since events using Viking data were selected for data quality. Images from Dynamics Explorer are also referred to. Like those of Viking, these are in the vacuum ultraviolet spectral region. These images have larger areal coverage but less resolution spatially and temporally than those of Viking. The more recent POLAR spacecraft provides images which are in a sense intermediate to those of Viking and DE, having less resolution in space and time than Viking but more than DE's spin scan camera. We now explore some details of these image sources.

1. Viking

The Viking spacecraft was launched on February 22, 1986 carrying a complement of instruments for investigating auroral and magnetospheric processes. It continued functioning into the late autumn of that year. Spacecraft instruments and initial scientific results were presented in a special section of the April 1987 issue of Geophysical Research Letters [volume 14, pages 379-482].

The imaging experiment, labeled V5, was based upon a pair of all-reflective f/1 cameras [Anger *et al.*, 1987b] with field of view 25°, that ended up slightly misaligned but which basically image the same field in two different vacuum ultraviolet passbands. Camera 0 passed 134 to 180 nm, mainly corresponding to emissions from the LBH bands of molecular nitrogen (N_2) and some from a line at 149.3 nm due to atomic NI. Camera 1 detected from 123.5 to 160 nm, where emission is largely due to neutral atomic oxygen (OI) multiplets at 130.4 and 135.6 nm, and to some of the LBH bands. Camera 1 ceased to function on May 5, 1986 [Vallance Jones *et al.*, 1987]. In principle the UV aurora could be observed on the dayside, but filters which allowed passage of longer wavelengths resulted in low signal to noise ratios in imaging these regions. Due to the ground station being in Kiruna, Sweden, and the use of only real-time, line-of-sight operation, imaging was restricted to the northern hemisphere. The effective exposure of an image is approximately one second and images could in principle be acquired on each spin of about 20 seconds. In practice, operation of several instruments in addition to V5 and bandwidth requirements often limited the imaging to about once per minute (the nominal time unit of this study due to availability of one-minute magnetic data).

UV images from Viking give an indication, on a 20-second to several minute timescale, of auroral luminosity, which in turn indicates regions of particle precipitation and thus current flow [Marklund *et al.*, 1987a]. An electrodynamic inversion method based on Viking images and Viking magnetic/electric data, along with observations from DMSP, was developed by Marklund and coworkers [1987b].

2. Dynamics Explorer

The Dynamics Explorers (DEs) were a pair of polar orbiting spacecraft on coplanar polar orbits [Fujii *et al.*, 1994]. DE 1 was launched in August 1981 and carried an imager. Its initial orbit had apogee above the northern polar cap at 3.63 R_e, enabling hemispheric views to be taken with 12 minute time resolution. DE 2 was on a much lower orbit, with apogee and perigee at 1012 km and 309 km.

By the time of the CDAW 9 events, some of which are discussed here, the DE 1 orbit had changed so that images were of the southern hemisphere. This study is based primarily on magnetic data from the northern hemisphere. The conjugacy of auroral forms between hemispheres may be used to remedy this situation, although such conjugacy should be used with care for both imaging and magnetic data. A case of good conjugacy, based on magnetic data, is discussed in Section 3.d. In such a case, by reversing the magnetic latitude in DE images, a northern hemisphere pseudo-image could be created. In practice, such images were of limited use in face of the greater spatial and temporal resolution from Viking images which were available for the CDAW events.

3. DMSP Imaging

The Defense Meteorological Satellite Program already referred to has consisted of a number of satellites carrying various instruments, with an imager being a constant feature due to its meteorological importance. Among the earliest satellite auroral images available, and sometimes accompanied by other data streams such as particles or magnetic perturbations, DMSP images have been used extensively in auroral studies. DMSP images are in the near infrared and visible. They are obtained in pushbroom fashion at relatively low altitude but show a nearly 3000 km wide strip of the Earth, although not all parts of the image are obtained simultaneously. During passages over the Earth's dark side the cameras are automatically adjusted to record images at low light levels, including auroral and man-made emissions. Due to low satellite altitude and the nature of the instrument, excellent spatial resolution is attained in DMSP images.

Image data for the relevant time periods being difficult to obtain, and given that for several of the events other imaging (or similar data) are used, DMSP images do not figure prominently in this study.

4. POLAR

The POLAR spacecraft carries 11 different science instruments of which the one of most interest here is the UV Imager (UVI experiment)[4]. POLAR was launched on February 24, 1996 into a 2 × 9 R_e polar orbit with a period of approximately 18 hours[5]. The CCD-based imager has a relatively narrow field of view of about 8 degrees (circular format) [Liou *et al.*, 1997]. Recent developments in UV imaging allowed the problems of contamination from

[4] http://www.geophys.washington.edu/Space/SpaceExp/POLAR/
[5] http://www-istp.gsfc.nasa.gov/istp/polar/polar.html

longer wavelengths, which occurred with Viking, to be largely circumvented, and the camera has good spatial resolution and a nominal frame rate of one per 37 seconds. Due to the higher apogee orbit, longer sequences of images (up to about 9 hours) are available from POLAR than from Viking. From typical imaging altitudes, the resolution at ionospheric height is about 30 to 40 km. As part of the International Solar-Terrestrial Physics project, POLAR data are available in near real-time to interested parties.

5. Meridian Scanning Photometry

Meridian scanning photometry data used are from the Meridian Scanning Photometer Array (MPA) instruments of the CANOPUS project [Xu *et al.*, 1993]. These instruments are located at Fort Smith, Pinawa, Gillam, and Rankin Inlet in western Canada (see map in Chapter 9). Meridian scans are taken through 8 filter wheels so that narrow passbands are seen centred at 557.7, 630.0, 470.9, 486.1, 480, 493.5, and 625 nm, the latter three of which correspond to background emissions, and the others to known auroral visible light emission lines [Rostoker *et al.*, 1995]. Using an assumed height of emission, the MPA data are generally presented as intensity versus latitude. In such a form they are well suited for comparison to results of the present project when used on magnetometer meridian chain data.

d. Magnetic Data and Electric Currents

The forward modelling technique used here makes a hypothetical link between observed quantities and their cause. In the case of inversion of magnetic fields, the hypothesis is that the effects observed are those due to electric currents flowing in the upper atmosphere and magnetosphere. The time scales considered are such that polarization effects (the displacement current term in Maxwell's equation) may be neglected. However, inductive effects may occur and induce currents (in the Earth most importantly) which in turn generate their own fields and complicate the relation of source currents to observed fields. Under certain assumptions, the forward model can incorporate such effects, and as used here that is done. Those assumptions may, however, be violated. This must be considered on a station-by-station basis. Earth induction is accounted for in the forward model under the assumption of an isotropic Earth, homogeneous in layers. In certain areas this may not be a very accurate representation of the true electromagnetic situation. For example, Icelandic stations have been found to have anomalous ratios of the vertical and horizontal components of the magnetic field [Hermance and Garland, 1968]. By comparison with Greenland data, taken as non-anomalous in regard to Earth induction, Icelandic data were found to have low values of Z/H in bay magnetic perturbations. Modelling indicated that the observed low ratios of Z/H could be explained by lava at 30 km depth, a not unreasonable hypothesis given the volcanic structure and activity in Iceland. For this study, this would indicate an anomalous situation not incorporated into the forward model and thus lead to inability to accurately model Icelandic data. As a control on use of Icelandic data here, it may be compared to conjugate data from the southern hemisphere. As shown in Figure 3.9, conjugacy between Husafell, Iceland, and Syowa, Antarctica, is excellent.

Figure 3.9 Conjugacy of Husafell and Syowa Stations. Husafell, Iceland data are shown by a solid line and those from Syowa, Antarctica by a dotted line. Z is at top, Y in middle, X at bottom. Time period shown is 0 UT to 10 UT April 3, 1986.

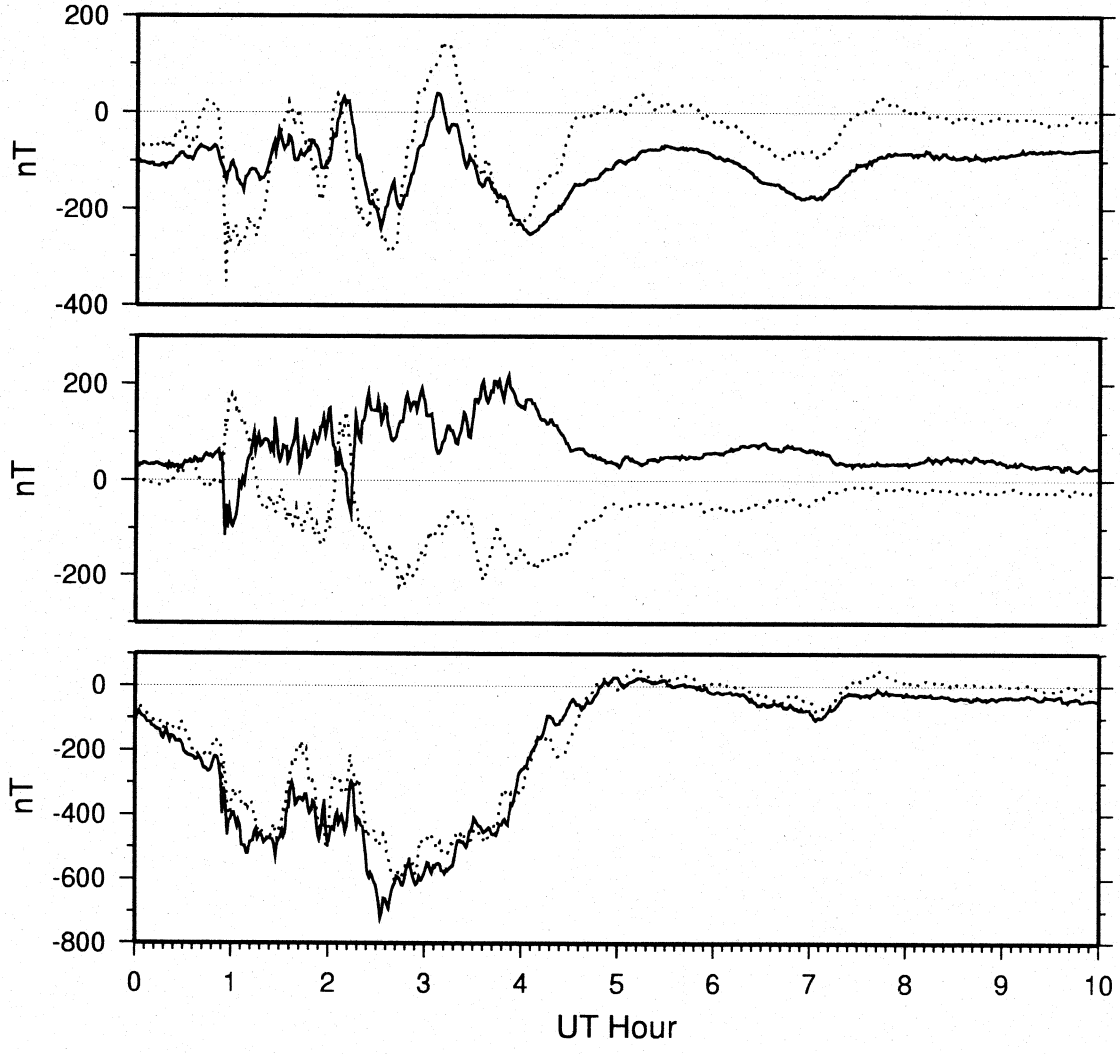

Two-second pulsation data from the XISY data set of the CDAW 9B were boxcar-averaged to one minute and referenced to a basetime of 20 UT April 2 1986 to produce this plot. The X components are almost identical. The Y components, arising from (primarily) north-south currents, are mirror images, showing that meridional current flow is oppositely directed but nonetheless highly negatively correlated. The Z components, which are sensitive largely to north-south positioning of the electrojets, are also a close match, although their sensitivity to exact conjugacy is greater than is that of the X component. Certainly no depression of Z/H ratios of a factor about 5 (as observed by Hermance and Garland) is evident. A comparison of data from Husafell and Syowa is also presented by Minatoya *et al.* [1996] shows only 'H' components, and a comparison is made to the more westerly Antarctic station Asuka. Surprisingly, although the changes in magnetic perturbations at Husafell and Syowa are highly correlated while those at Asuka

appear to have a time lag, comparison of auroral forms suggested that those at Asuka were the more nearly conjugate with Husafell. The conclusion was that the conjugacy was distorted longitudinally, presumably due to field-aligned current effects. The relevance here is simply to reinforce the idea that care must be taken in use of conjugate data.

Conjugate data appear to indicate that Icelandic stations are not in fact greatly affected by deep structure. There remains the possibility of local anomalies (also often associated with volcanic regions) affecting Icelandic data. This may also be considered and dismissed for Husafell by comparing its data to those from the nearby magnetometer at Leirvogur. The magnetograms from these two stations, separated by about 20 km, were compared: the records at the two stations are basically identical and show little evidence of local anomaly. For these reasons Icelandic data will be considered as fully useable in this study.

A further use of conjugacy is to fill in gaps in station distribution. In practice there are not enough stations in the Southern Hemisphere (partly due to sparse population density and partly due to the distribution of oceans) for modelling techniques to be applied there. While the situation is better in the Northern Hemisphere, there are still regions where stations are sparse. That the high degree of conjugacy shown in Figure 3.9 is due to similarity of the physical conditions is dramatically reinforced by Figure 3.10, which shows conjugate auroral forms of a very great similarity. One might thus consider developing rules for transforming Southern Hemisphere data for use in modelling in the Northern Hemisphere. Inspection of Figure 3.9 shows that for conjugate stations simply a reversal of sign of the Y or D (east-west) perturbation is needed to make data correspond across hemispheres. This is physically reasonable as that component primarily responds to meridional currents and poleward flow (i.e. symmetric meridional flow) in each hemisphere produces a reversed sign of toroidal perturbation. The X or H component of an electrojet flowing east-west would be expected to be relatively insensitive to exact conjugacy whereas the Z component, at least near the centre of the electrojet, has a steep gradient and thus would lose coherence quickly in response to deviations from exact conjugacy. Inspection of Figure 3.1 will verify that these are indeed the observed behaviours. This aspect of conjugacy could be used in two ways: either to present more data to the modelling routine, or more conservatively to demonstrate the validity of the modelling routine by calculating fields from the model parameters and then comparing them to those observed at conjugate stations. The latter, more conservative approach is used here. Figure 3.11 shows the relatively few existing conjugate station pairs and some important regions: Halley and the north-west tip of Newfoundland; Syowa and Iceland; Siple and Roberval, Québec; and South Pole to Iqaluit on Baffin Island [Lanzerotti *et al.*, 1991].

Figure 3.10 Photographs of aurora simultaneously taken at conjugate points. A high degree of correlation among auroral forms is seen. From Rycroft [1987].

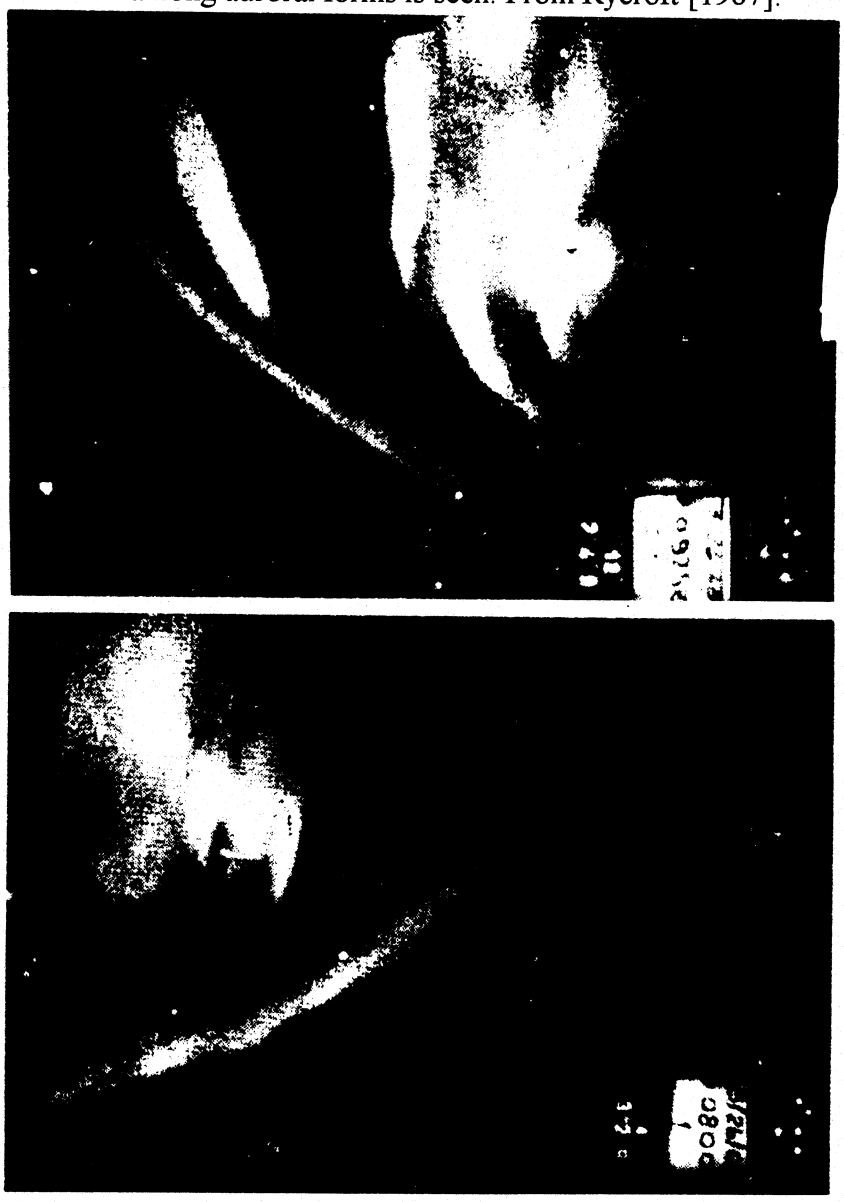

Quite apart from use of conjugate data to fill station gaps, they may be used with less weight to verify the accuracy of modelling results. Particularly at times when the existence of good conjugacy is established through use of observations such as those presented in Figure 3.1, accurate representation of the currents in one hemisphere should allow calculation of magnetic fields in that hemisphere, or, subject to the transformations and assumptions presented above, those at any postition in the opposite hemisphere. A good verification of the physical reality of parameters derived in this study would be considered to be the calculation of a conjugate station's observations from parameters derived through the modelling.

Figure 3.11 Superposed northern and southern hemisphere maps showing conjugate stations. From Lanzerotti *et al.*[1991].

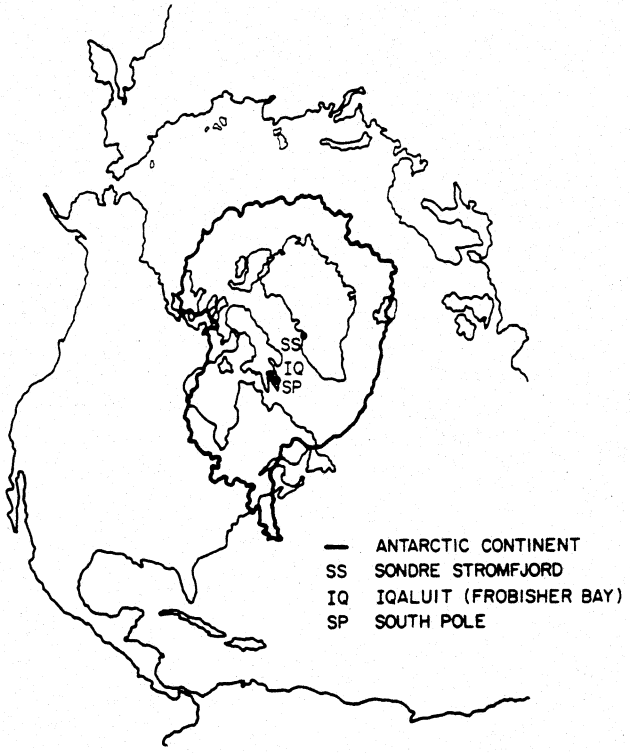

It is briefly noted that the limited use of conjugacy is not restricted to this study. The AMIE procedure (see Section 4.b), which takes estimates of conductivity data as an important input, uses southern hemisphere data [Knipp, 1989, p. 23], but assigns a lower statistical weight to such cases. Conjugate data for satellites are important in this regard since conjugate data may be the only way to fill in a gap at a given time and local time. Even in cases where the satellite crosses the desired local time in the northern hemisphere, it may do so at a time when conductivities may have varied. Then the use of conjugate data for the time in question may introduce less error than use of northern hemisphere data from an inappropriate time.

e. Coordinate Systems and Transformations

A number of coordinate systems are used in geomagnetism. Certain systems associate naturally with certain problems, but while this association may simplify the problem at hand, comparison to other aspects of the problem, perhaps better studied with a different coordinate system, may become difficult.

In the very good approximation that the Earth is spherical, a geodetic system related to the rotation axis of the planet and some other fixed reference point may be adopted. The standard geodetic system is based on the latitude, that is, the angle subtended at the centre of the Earth between the Equator and a point, and the longitude, which is the angle between the defined zero meridian and that of the point, as measured along the Equator. The latitude is positive in the northern hemisphere and negative in the southern hemisphere. Longitude is positive if the shortest angular distance to the meridian of a point

is obtained by going eastward from the zero meridian, which is defined to be that of Greenwich, England, and negative otherwise. Longitude may also be defined as varying from 0 to 360 degrees going only eastward, in which case it is often referred to as east longitude. It is sometimes useful to speak of the colatitude of a point, which is, in degrees, 90 minus its latitude. This coordinate is analogous to the polar angle in standard spherical coordinates.

The simplest analogous magnetic coordinate system is obtained by defining polar points and a standard meridian and considering angles analogous to the latitude and longitude to be the magnetic latitude and magnetic longitude. This system is useful as the internally generated field of the Earth is dominated, in a spherical harmonic expansion in a Cartesian system based on the centre of the geodetic system, by the dipole term [Langel, 1987]. The coordinate system thus defined is referred to as the dipole coordinate system, or geomagnetic coordinate system. In order to differentiate it from other dipole-based systems, the adjectives tilted, oblique, and/or centred are often used. This will be the primary coordinate system used here and it is here referred to as the centred dipole system. A major aspect of the choice of coordinate system is that the problem should be well represented in it: operational concerns may dictate that the problem be adequately represented while not requiring undue computational baggage. The centred dipole system is orthogonal, easily related to the geodetic system by rotations, and has a simple representation of field lines along which currents may flow. Its suitability for geomagnetic modelling, at least on a regional scale, has been demonstrated in the studies of Kisabeth [1972, 1979] and Kisabeth and Rostoker [1973, 1977]. The definition of the magnetic poles required in order to define the centred dipole coordinate system in practice amounts to specifying the geodetic location of the north magnetic pole. That pole location is not constant but varies, for reasons which remain unclear (as indeed does the entire mechanism by which the Earth's internal field is generated). Although this variation has been small since about 1900, in principle the pole location should be calculated from empirical formulae, as a first step in defining the centred dipole coordinates. In 1980 the geodetic coordinates of the north magnetic pole were latitude 78.8° N, east longitude 289.3° [Langel, 1987]. By April 1986, the position as calculated from routines of Hapgood [1991] was latitude 78.85°, east longitude 289.1°. Pole positions calculated from formulas given by Hapgood [1991], appropriate to the date in question, are used throughout this thesis.

Within both of the coordinate systems defined above, vectors may be represented in local Cartesian systems. The local geodetic system is conventionally defined with an axis X directed northward, an axis Y directed eastward, and a Z axis completing a right-handed system by being directed vertically downward. Components of the magnetic induction in the local geodetic system are usually referred to simply as the X, Y, and Z components. Another common way of describing the magnetic field at a given location is to emphasize its strength and declination. In the World Data Center system, also used by the United States Geological Survey, H is the horizontal intensity in nT, D the declination (an angle), and Z the vertical intensity. Z is identical to the Z component in the local geodetic system and is positive downward. H is the modulus of the vector sum of the geodetic X and Y

components. The direction of these horizontal components is expressed as the declination angle D (often given in minutes of arc or degrees) between them and the geodetic X axis, measured eastward. The conventional HDZ specification of the field does not directly specify a vector since D is in fact an angle. A useful vector quantity, due to the observed ordering of currents by the geomagnetic field, is the representation of the field in a local geomagnetic system. By analogy to the practice for the geodetic local system, the magnetic induction components can be referred to as X_M, Y_M, and Z, with the Z component identical to that of the local geodetic system. In this study, unless indicated otherwise, X_M, Y_M, and Z components are in a local Cartesian system based on the centred dipole main field model. The X_M axis is taken to be parallel to meridians in the centred dipole coordinate system, while the Y_M axis is directed magnetically eastward (lies 90° clockwise from the X_M axis when facing radially inward). Components in the local Cartesian systems are related to one another through appropriate rotations. There is a loose practice of using the terms H, D, and Z for what is here referred to as X_M, Y_M, and Z. It is important to know the units accompanying magnetic data to avoid confusion. Another variant is to use HDZ, sometimes referred to as HEZ to indicate that the eastward value is not an angle, as the axes in a truly local coordinate system established by orientation of a magnetometer on a quiet day. Such local magnetic components will sometimes be used in what follows: if this is what is supplied by a data source it is not always possible to transform to the true centred dipole (or any other) system. For modelling in such a case, it has to be assumed that the local and centred dipole systems do not dramatically differ. Alignment with local magnetic coordinates is often done for campaigns, especially for pulsation data in which absolute directional accuracy is not essential (see for example Lanzerotti *et al.* [1991]). The true declination of a site is based on local magnetic measurements, usually made through aeromagnetic surveys, and reflects higher-order terms in an expansion of the true observed field (including local anomalies due to ore bodies, etc.). Such a declination is required to convert a compass reading, for example, to true north, and is usually given on maps along with an epoch and annual variation. Global maps of declination (variation) are available (e.g. U. S. Navy Hydrographic Office [1965], or see Forbes [1987] or Langel [1987]).

The centred dipole system is based on only one term in a multipole expansion of the Earth's internal field. Field models incorporating higher orders may also be used to define coordinate systems. The most commonly used such system is the corrected geomagnetic system (CGM) of Gustafsson [1983; see also reference therein]. Like the centred dipole system, this coordinate system changes as the components of the multipole change slowly with time. Unlike that system, corrected geomagnetic coordinates do not form an orthogonal system and are in fact defined numerically. Lines of constant corrected geomagnetic latitude result from the tracing of field lines from a circle in the dipole equatorial plane to the surface. The field lines are the tangent lines of the magnetic field supplied by the chosen model field (which is usually the IGRF standard model appropriate for the epoch). While the corrected geomagnetic system has found many applications and its lines of constant latitude seem to form a good system for organizing magnetic data, here the complications involved in its use are not likely to be worthwhile. Below, certain data sets may be presented in corrected geomagnetic coordinates, but it will be made clear

in appropriate places that comparisons to the modelling results, presented in centred dipole coordinates, must be undertaken with care. The two coordinate systems do not differ dramatically. Nevertheless, special care must be used in comparison of corrected geomagnetic coordinates to centred dipole coordinates in certain longitudinal sectors. This is illustrated by Figure 3.12, which shows that there may be as much as about 5° of difference between the two systems in the 60° to 120° geomagnetic longitude sector (northern Europe). While centred dipole curves are the result of a coordinate rotation and vary smoothly, between the geodetic latitude minus the dipole tilt (about 11°), to the geodetic latitude plus the dipole tilt 180° away, the corrected geomagnetic curves have a complex although basically similar dependence on longitude. The form of the curves illustrates the dependence of the corrected geomagnetic coordinates on higher-order terms in the expansion of the Earth's field: at places the corrected latitude has opposite curvature with longitude to that of the one-term centred dipole approximation.

Figure 3.12 Curves of CGM and centred dipole latitudes as a function of geodetic longitude. Solid curves are CGM latitudes corresponding to geodetic latitudes of (from top) 80°, 70°, and 60°, with geodetic longitude varying. Nearest dotted curve to each is the corresponding centred dipole latitude curve.

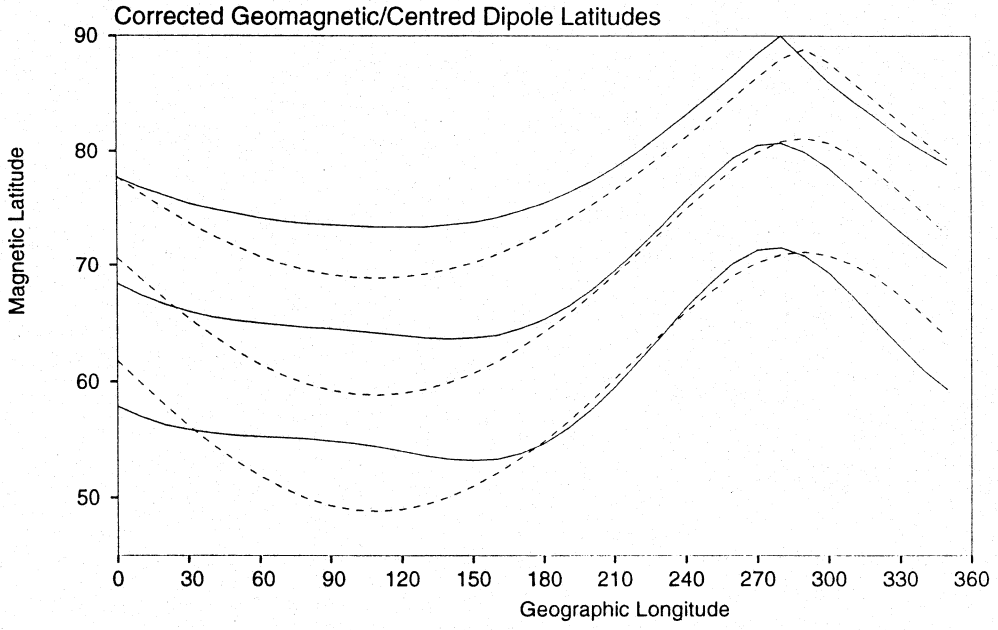

In practice corrected geomagnetic coordinates are obtained by interpolation in a table such as that supplied by Gustafsson [1983]. Spacecraft data may be referred to the corrected geomagnetic system by tracing from the spacecraft location to the ionosphere in geodetic coordinates (since routines to calculate IGRF field values usually take as input geodetic coordinates and since spacecraft ephemerides are also calculated in that system). A transformation is then made from the ionospheric 'foot' position to corrected geomagnetic coordinates. Ephemerides of the DMSP satellite provide both geodetic coordinates and corrected geomagnetic footprint coordinates computed in this way [F. Rich, personal

communication to G. Rostoker, 1991]. In this study the geodetic coordinates of the footprint were converted to centred dipole geomagnetic coordinates, which is thus a consistent system in which to present results. As discussed in section 3.a.1.c, the spacecraft data are given in a coordinate system moving with the spacecraft and must be transformed to an Earth-based system. This transformation is a rotation through an angle which varies with the spacecraft position, much as the transformation from local geodetic to centred dipole coordinates is a rotation through the centred dipole declination, which varies with location.

As more particularly discussed in section 3.a.1.c, DMSP data are supplied with an ephemeris specifying the footprint position in geographic coordinates and in the corresponding corrected geomagnetic coordinates. Since the present study uses centred dipole geomagnetic coordinates, the most appropriate coordinate system to use for comparison of spacecraft observation with results of ground-based modelling are not in fact supplied by the ephemeris. For this reason, the geographic coordinates of the footprint were transformed into the centred dipole system. It was verified that there was only a small difference between the centred dipole coordinates computed in this manner and the supplied corrected geomagnetic coordinates. Figure 3.13 illustrates the path of the spacecraft by showing the footprint positions, at one minute intervals, for a northern hemisphere pass of the DMSP F7 spacecraft on April 2 1986 (860402) from 2320 to 2350 UT. The top panel shows the spacecraft trajectory in geographic coordinates with continental outlines shown for reference. Bottom panel shows the spacecraft trajectory in magnetic coordinates with the centre of the diagram being at magnetic longitude zero, magnetic latitude 70°. Corrected geomagnetic coordinates from the ephemeris file are used to produce the path marked by white dots (initial point marked in black). The nearby grey path is the path in centred dipole coordinates as used in this study. V-shaped path at the right indicates the corrected geomagnetic midnight position during the trajectory by showing coordinate pairs of midnight longitude and spacecraft latitude. The spacecraft passes midnight about four fifths of the way through the pass as would be expected from the geographic position and the UT. For the same pass, Figure 3.14 illustrates the corrected geomagnetic latitude at one minute intervals, the corresponding centred dipole latitudes, and the smooth interpolating curve which provides centred dipole coordinates at any time. The centred dipole-corrected geomagnetic differences are within the expected range and the interpolation of coordinates works in a smooth manner and is seen to accurately reflect the ephemeris information. It is noted in passing that cyclic coordinates (longitudes or local times) must be converted to continuous functions before interpolation. For example, magnetic local time for the trajectory shown in Figure 3.13 would change discontinuously in the ephemeris from above 0 h to nearly 24 h as the spacecraft passes through local magnetic midnight. Before interpolation it is essential to convert this to a smooth function, which in this case would result in a value passing from above 0 h to negative values.

Figure 3.13 Coordinates of DMSP F7 satellite footprints on a northern hemisphere pass. Top figure shows geodetic, bottom magnetic footprints. See text for details.

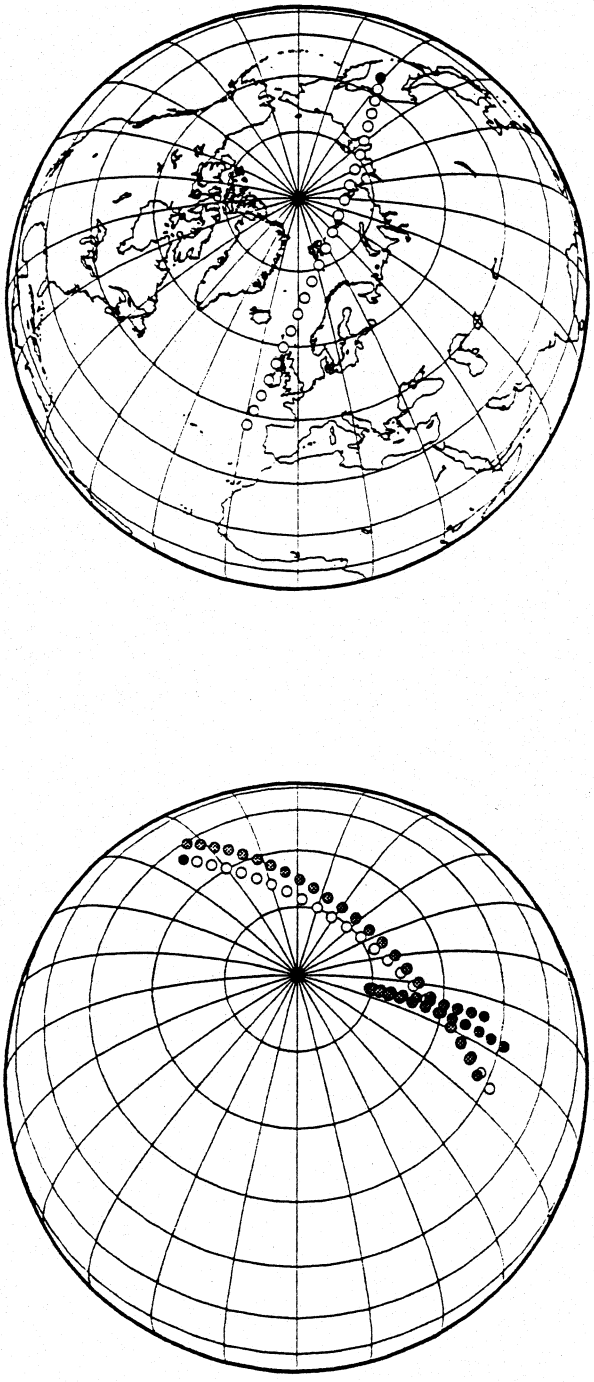

Figure 3.14 Latitude of DMSP F7 spacecraft on April 2 1986. CGM latitude of the spacecraft footprint is shown by line segments with time spacing one minute. Corresponding centred dipole latitudes, as calculated from the geodetic coordinates in the ephemeris file, are shown by dots at one minute intervals. Latitudes assigned by interpolation are shown by a solid curve which passes through the dots.

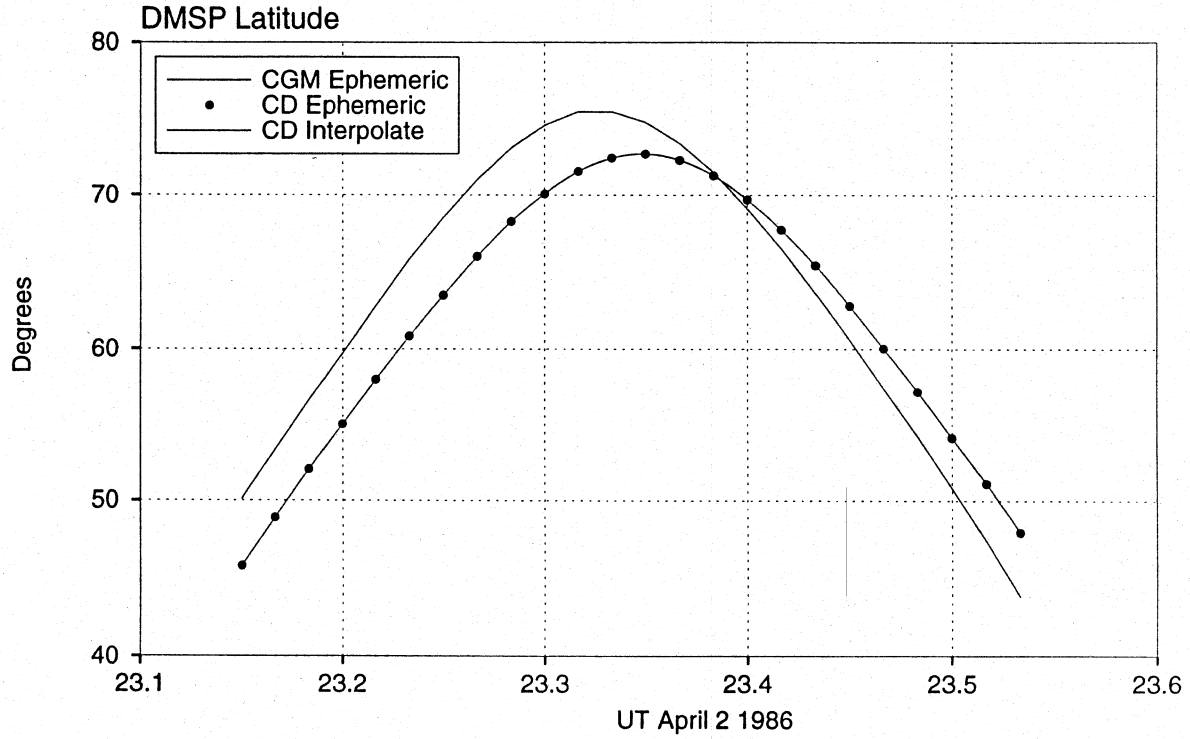

Given the role of the solar wind in forming the magnetosphere, it has been observed that magnetospheric structure and events are to a large degree ordered by the angle from the Sun-Earth line, which is conveniently expressed as a time. The subsolar point is readily calculated given the coordinates of the Sun and the orientation of the Earth. The coordinates of the Sun are obtained from a solar ephemeris while the orientation of the Earth may be expressed through the sidereal time at Greenwich. Both are standard calculations in positional astronomy [Duffett-Smith, 1990]. The antisolar point is 180° in longitude from the subsolar point and at the negative of its latitude. The geomagnetic coordinates of the antisolar point may be calculated in the desired coordinate system and the difference between the magnetic longitude of any point and that of the antisolar point, expressed in hours, is the magnetic local time (MLT). One hour of MLT is equivalent to 15° of longitude. The several types of MLT possible differ significantly only in the polar regions. In this study, unless otherwise specified, the centred dipole MLT is used.

Yet more near-Earth coordinate systems may be defined to reflect aspects of the geomagnetic field and the phenomena which it influences. Viking images are generally presented with eccentric dipole coordinates (EDFL). Invariant coordinate systems may be defined based on aspects of particle motion and are useful in meridian scanning photometry and in organizing particle data. In a dipolar field the invariant system is identical to 'centred dipole coordinates' and the two terms will sometimes be used interchangeably in what follows. In practice the advantages that the specialized coordinate systems lend to certain restricted studies will not be evident here. The many possible systems can be confusing, and here an attempt will be made to refer all data to the centred dipole system.

Brief mention must also be made of systems used for 'magnetospheric' spacecraft. The outer magnetosphere is more strongly organized by the solar wind and its interaction with the dipole than by the dipole alone. Since the solar wind flow (but not field) is largely radial, useful systems are based on the Sun-Earth line. The two most commonly used such systems are Cartesian with differences in choice of the orthogonal axes. They are the Geocentric Solar Ecliptic (GSE) and Geocentric Solar Magnetospheric (GSM) systems. Both have the X axis pointing from the Earth to the Sun. In GSE, the Y axis is in the ecliptic plane pointing toward dusk and the Z axis is pointed toward the ecliptic pole. The GSM system is useful for roughly showing the effects of the angle of the Earth's dipole in the solar wind. Its Z axis is antiparallel to the projection of the dipole into the plane perpendicular to the X axis, and the Y axis is the second component of an orthogonal triad. Transformations between these systems are described by Russell [1971], Hapgood [1991], and Appendix 2 of the recent book edited by Kivelson and Russell [1995].